

# On Stress-Relaxation Experiments and Their Significance Under Strain-Aging Conditions

MARC A. MEYERS, J. R. C. GUIMARÃES, AND R. R. AVILLEZ

Two simple tests are presented to verify whether the mechanical response of the substructure remains constant during stress relaxation. They consist of a) subjecting the sample to repeated relaxation cycles from the same reference load and b) reloading the sample after the last cycle. Either exhaustion of relaxation after repeated cycles or yield-point formation on reloading are indicative of a decrease in the mobile dislocation density. Accordingly, a method is developed for the determination of the time dependence of the mobile dislocation density, using the decrease in relaxation rates in repeated cycling. The exhaustion of relaxation in Armco iron is found to be in good agreement with predictions for the decrease of mobile dislocation density by a pinning mechanism.

## 1. INTRODUCTION

STRESS-relaxation experiments have been extensively used to obtain parameters of microdynamical deformation processes in metals and alloys. Among these the most common are the internal and effective stresses,<sup>1-3</sup> and the activation volume.<sup>4</sup> The analysis of stress-relaxation experiments can be carried out along two different paths: using an empirical relationship between stress and dislocation velocity, such as Johnston and Gilman's<sup>5</sup> (e.g., Refs. 1 and 2) or using the theory of thermal activation processes (e.g., Ref. 4). These two alternate routes are described by Krausz.<sup>6</sup> The conventional methods for the analysis of stress-relaxation results of metals and alloys are based on one assumption: that the substructure and barriers remain unchanged during the test. The failure of one of these assumptions would render any parameter obtained therefrom of doubtful value. This is considered upsetting since there are evidences in the literature that the mobile dislocation density varies during relaxation.<sup>7-12</sup> Rohde and Nordstrom<sup>7</sup> presented evidence showing that the dislocation substructure underwent changes during relaxation. Specifically, they observed a decrease in mobile dislocation density,  $\rho_m$ , during relaxation, of the form:

$$\rho_m = \rho_m(0)e^{-\theta\epsilon_{pr}} \quad [1]$$

where  $\theta$  is an immobilization parameter,  $\epsilon_{pr}$  is the plastic strain during relaxation, and  $\rho_m(0)$  is the mobile dislocation density at the beginning of the relaxation transient. Equation [1] could be used to correct the conventional methods for the analysis of relaxation data, if  $\theta$  were determined. But, according to Rohde and Nordstrom<sup>7</sup> there is no independent means of obtaining  $\theta$ . Recently, Okazaki *et al.*<sup>13</sup> presented a method for the analysis of stress-relaxation results assuming a variable dislocation density. However, their function

describing the variation of mobile dislocation density is rather arbitrary, since it is based on the deviation of the results from a pre-established equation (Johnston-Gilman<sup>5</sup>).

Both the observation of the material behavior during repeated relaxation cycles<sup>10,11</sup> from the same initial load and the analysis of the reloading stress-strain curve after relaxation<sup>12</sup> have been suggested as suitable for detecting changes in the mechanical response of the substructure of the material. Either "exhaustion" or the development of a complex reloading yielding after repeated relaxation cycles would be indicative of substructure evolution during the foregoing stress relaxation.

Accordingly, this paper has the following objectives: a) to present two tests—namely, repeated relaxation and reloading after relaxation—conducted on copper, 6061-T6 aluminum, Armco magnetic ingot iron, and an Fe-31 pct Ni-0.1 pct C (wt pct) alloy to verify whether the mechanical response of the substructure remained constant during relaxation, and b) to propose a method for the determination of the time dependence of the mobile dislocation density, and to use it to determine deformation parameters. It should be emphasized that the principal objective of this study was not to investigate in detail these systems; rather, they are used to illustrate the changes in the mechanical response of the substructure, as well as the correction methods developed. Consequently, no attempt was made to exhaustively investigate these alloys nor to systematically determine the various fundamental deformation parameters.

## 2. REPEATED RELAXATION AND RELOADING EXPERIMENTS

In the past, the majority of stress relaxation tests were conducted in screw-driven tensile testing machines. These machines are amenable to relaxation themselves and its effect has to be determined and, if significant, subtracted. To the authors' knowledge, machine relaxation has not been correctly accounted for in the past. The method most commonly used consisted of replacing the specimen by a block with larger cross-sectional area and high yield stress, so that loading to the same loads than the specimen results only in elastic stress. If the specimen length can

MARC A. MEYERS is Assistant Professor, Department of Metallurgical Engineering, South Dakota School of Mines and Technology, Rapid City, SD 57701. J. R. C. GUIMARÃES is Professor, Center for Materials Research, Instituto Militar de Engenharia, Rio de Janeiro-RJ-Brasil. R. R. AVILLEZ, formerly Graduate Student, Center for Materials Research, Instituto Militar de Engenharia, is now Graduate Student, Department of Metallurgy and Mining Engineering, University of Illinois at Urbana-Champaign, Urbana, IL 61801.

Manuscript submitted April 11, 1978.

be reduced to a minimum for this purpose, relaxation is further reduced; all relaxation can then be attributed to the machine. The common error comes from the fact that the corrections were made using the same crosshead velocity for both "dummy" sample and specimen. Guu and Pratt<sup>13</sup> found—and this was confirmed in the present investigation—that the amount of machine relaxation was negligible at very low crosshead velocities but became important at higher crosshead velocities. But the machine does not "know" whether a "dummy" sample or specimen is being loaded and relaxed. The important parameter determining machine relaxation is probably the rate of increase of load; if it is low, relaxation is very small, once the crosshead is stopped. On the other hand, if the rate of increase of load is high, this accommodation cannot take place. This is due to the fact that at low crosshead velocities relaxation can take place concurrently with loading, so that relaxation after the crosshead is stopped is reduced. The rate of increase of load is given by the elastic curve, when the "dummy" sample is being used. On the other hand, the work-hardening rate determines the rate of increase of load for the specimen being plastically deformed. The conclusion is that the "dummy" sample should be tested at crosshead velocities providing rates of load increases equal to the ones in the specimen, just prior to relaxation initiation. Another observation made in the course of the present investigation is that hand-tightened wedge-action grips introduce extensive relaxation. This was verified by comparing the relaxations after two different sequences; letting the system (with "dummy" sample) relax, unloading, reloading, and stopping the crosshead for the second time; no relaxation was observed. On the other hand, when the "dummy" sample was loosened and retightened after unloading, and then reloaded and re-relaxed, relaxation was essentially the same as for the first cycle. Consequently, a considerable amount of the relaxation was concentrated at the grips. These grips should therefore be avoided. If not possible, the "dummy" sample should have the same hardness and "bite" area as the specimen.

All the above difficulties contribute to cast a doubt on the validity of the stress-relaxation data obtained from mechanical testing machines. Fortunately, in the newer servohydraulic machines, that can be operated under strain control with strain-gage extensometers, these problems are circumvented. Stress relaxation is obtained under conditions of constant total strain (zero total strain during relaxation); the machine stiffness is infinite and its relaxation is zero. So, the plastic strain undergone by the specimen during relaxation is equal (but opposite in sign) to the elastic strain. This can be inferred from Eq. [2] of Guu and Pratt.<sup>13</sup> The tests described in this section (except the ones for the Fe-31 pct Ni-0.1 pct C alloy) were conducted in a MTS universal testing machine, under strain control mode, controlled by a 0.5 in. MTS strain-gage extensometer (Model 632.133 20) attached to the sample. The tests were conducted at 298 K and the sample was protected from air currents by means of a styrofoam box. For one experiment, the total strain was recorded as a function of time during relaxation. It was found, as expected, to be constant

within the experimental error (zero total strain during relaxation). Different strain rates were used in the different experiments; they are given in Figs. 1 to 3.

Figure 1 shows the three stress-relaxation experiments conducted in a cold-worked copper sample (99.999 pct purity, cylindrical specimen with cross-sectional area of 15.9 mm<sup>2</sup>). Practically no exhaustion was observed and the tensile curve does not show any abnormality on reloading. These features should be indicative of a constant mobile dislocation density. The above results are not consistent with Lloyd and Embury's<sup>11</sup> experiments. However, no mention of correction for machine relaxation is made in their paper, and the "exhaustion" that they observed in copper at 273 K could be due to machine effects. An attempt at determining the internal stress by incremental unloading was made; it is shown in the right side of Fig. 1. No "upward relaxation" could be observed. This is indeed interesting, since the "negative" (or upward) relaxation has been used in the past to determine the internal stress (*e.g.*, Gibbs<sup>14</sup>). This suggests that the "upward" relaxation could be a machine effect. The authors think that this point deserves further clarification.\*

\*Additional experiments at ambient temperature, using conditions and load decrements similar to K. Okazaki, Y. Aono, T. Kaneyuki, and H. Conrad<sup>14</sup> and conducted on cold-worked copper specimens failed to disclose any "upward" or "negative" relaxation. If present, this "negative" relaxation is beyond the detection sensitivity of the MTS under strain control.

Figure 2 shows the stress-relaxation sequence for 6061-T6 aluminum (shoulderless cylindrical specimen with cross-sectional area of 70.9 mm<sup>2</sup>). The abscissa represents time; it goes from zero to sixty min. The plot was divided into three parts and stacked vertically, for clarity. Successive stress-relaxation experiments were performed at three plastic strains: 0.0085, 0.025, and 0.04. Both exhaustion and reloading yield points could be observed at the three strains. In all cases the flow stress after the relaxation cycles was higher than the stress from which the sample was relaxed. This can be inferred from the horizontal dashed lines drawn in Fig. 2. At the plastic strain of 0.04, the stress just overcame the flow stress, for the second cycle (top third of Fig. 2). The relaxation for this cycle was more pronounced than the second relaxation cycles at the plastic strains of 0.0085 and 0.025. This shows that part of the immobilized dislocations was unlocked in the process. The results of Fig. 2 provide an alternative interpretation for

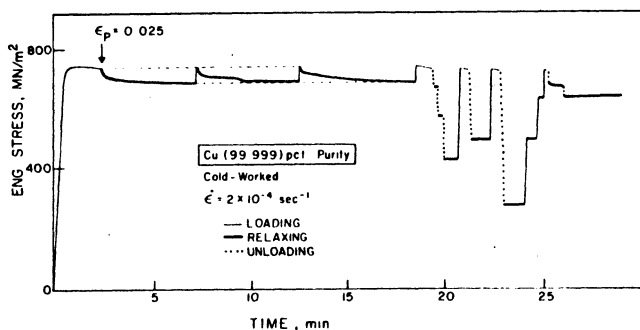


Fig. 1—Sequential relaxations for copper. Notice also, in the right hand corner, an unsuccessful attempt at obtaining "negative" relaxation, when stress is below internal stress. MTS under strain control.

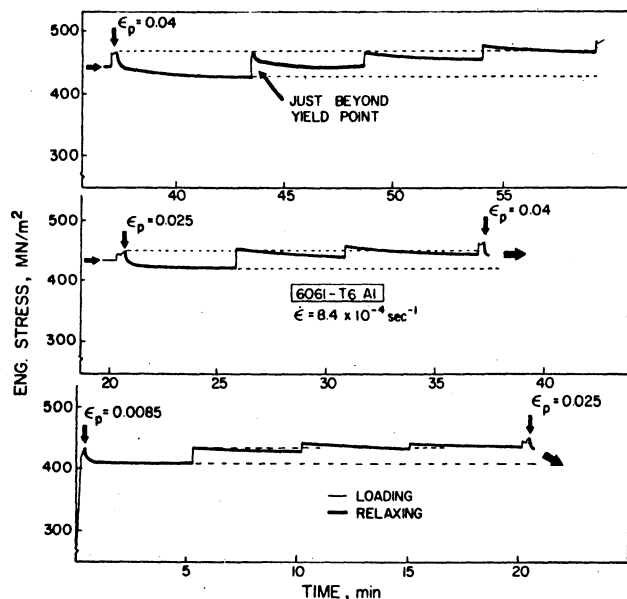


Fig. 2—Sequential relaxations for 6061-T6 aluminum. MTS under strain control.

Gillis and Medrano's<sup>15</sup> results. They used the angle between the tangents to the plastic curve and the relaxation curve, at the onset of relaxation, to determine the machine stiffness. For 6064-T6 aluminum, they subjected the sample to a series of relaxations up to a plastic strain of 0.01. The angles varied widely and they attributed these variations to changes in machine stiffness from relaxation to relaxation. The results shown in Fig. 2 show incontrovertibly that the changes in the initial angle are due to changes in the mechanical response of the substructure of the sample; in the strain-control mode under which it was operating, the stiffness of the MTS was infinite.

Figure 3 shows a plot similar to the one in Fig. 2 for Armco magnetic ingot iron. The chemical analysis revealed the following components (in wt pct): Al-0.07, C-0.006, Cr-0.05, Cu-0.11, Mn-0.14, Mo-0.04,

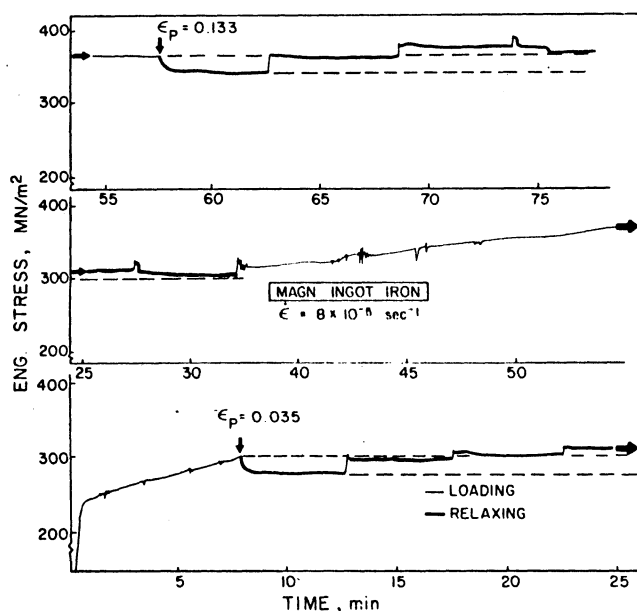


Fig. 3—Sequential relaxations for Armco magnetic ingot iron. MTS under strain control.

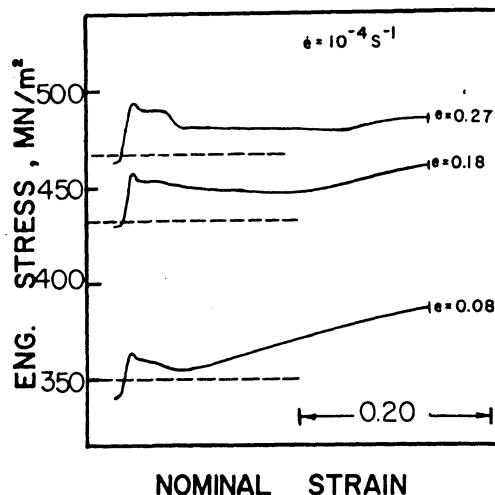


Fig. 4—Reloading curves after three one-hour relaxation cycles for an Fe-31 pct Ni-0.1 pct C alloy, at nominal strains at 0.08, 0.18, and 0.27. The dashed lines indicate the stresses from which the sequential relaxations were conducted. Data obtained from screw-driven Instron.

Ni-0.07, N-0.006, O-0.004, P-0.006, Si-0.08, S-0.019, Ti-0.07. The sample was machined from 2.8 mm thick sheet, annealed at 973 K for 16 h in a protective salt bath, quenched in oil, and tested at ambient temperature approximately thirty min after removal from the salt bath. Repeated stress relaxations of five min each were conducted from the plastic strains of 0.035 and 0.133. The exhaustion of relaxation was dramatic, as shown by the dashed lines. After the first cycle (5 min) the relaxation was practically exhausted. In the fifth cycle of the first relaxation series ( $\epsilon_p = 0.035$ ) the stress suddenly dropped during relaxation. This drop occurred again, twice, during the fourth cycle of the second series ( $\epsilon_p = 0.133$ ). Upon reloading the sample after the first relaxation series, there is a yield point formation. Irregularities in the plastic region of the curve were noted. It is not known whether they are due to the breaking-off of a thin oxide layer or whether they are caused by substructural interactions in the bulk of the sample. They are reproduced in Fig. 3.

The same type of experiments was performed for a Fe-31 pct Ni-0.1 pct C (wt pct) alloy using an Instron TT-DM universal testing machine (using handtightened alligator grips). The results are discussed in greater detail elsewhere.<sup>16</sup> Both exhaustion and yield point formation were observed. Figure 4 illustrates the nature of the reloading yield points, obtained after three one-hour relaxation cycles at the strains indicated. The dashed line indicates the stress from which the relaxations were conducted. In all cases the curves exhibited three characteristic stages: a yield point, followed by a plateau and an intermediary softening region, and finally the return to the original trajectory. The magnitude and length of these stages were affected by the predeformation and number of relaxation cycles; however, a clear yield point was always observed. From the dashed lines in Fig. 4 it can be seen that the flow stress after relaxation was always higher than before. It should be noted that Bolling<sup>17</sup> found yield points in several fcc metals and alloys. He induced yield points by several means, including aging under stress, unloading, and combinations

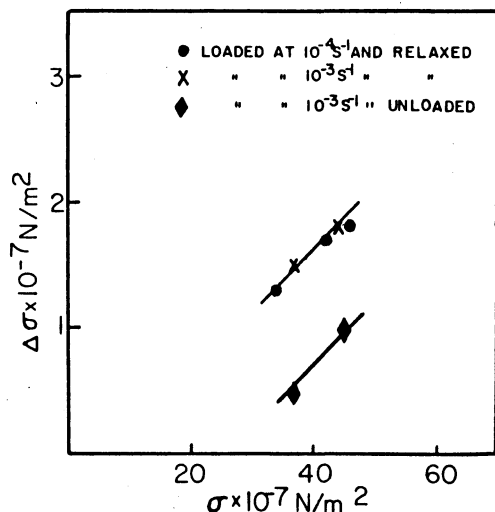


Fig. 5—Overstress  $\Delta\sigma$  (nominal stress at peak of yield point minus stress from which relaxation was conducted) vs stress  $\sigma$  from which relaxations were conducted; conditions (x) and (●) correspond to specimens loaded at a nominal strain rate of  $10^{-4}$  and  $10^{-3}$  s $^{-1}$ , respectively, and relaxed for one h; condition (♦) corresponds to a strain rate of  $10^{-3}$  s $^{-1}$  on loading and maintaining the specimen unloaded for one h. Data obtained from screw-driven Instron.

therefrom. Additional evidence of processes occurring during relaxation capable of affecting the mechanical response of the substructure are given in Fig. 5. The over stresses (flow stress on reloading minus stress from which relaxation was conducted) after one relaxation cycle (one hour) were plotted against the initial load, for tests conducted at two nominal strain rates ( $10^{-3}$  and  $10^{-4}$  s $^{-1}$ ). The over stress (or yield increment<sup>18</sup>) increases with prestress. Roberts and Owen<sup>18</sup> did not find such a dependence for high carbon martensite in an Fe-18 pct Ni-0.1 pct C alloy, but their highest prestrain was 0.03, while the prestrains in Fig. 5 went up to 0.27. The second set of points of Fig. 5, represented by diamonds, shows the over stress after unloading, maintaining the sample at zero load for one h, and reloading it. It can be seen that the over stress is only 50 pct of the over stress due to relaxation. This behavior is consistent with Bolling's<sup>17</sup> results.

Magee and Paxton<sup>19</sup> observed exhaustion of relaxation for an Fe-31 pct Ni alloy partially transformed to martensite; they interpreted it as being due to transformation of austenite into martensite during reloading (from  $n$ th cycle to  $(n+1)$ th cycle). However, in the experiments conducted by us the alloy was fully austenitic and so remained during the whole extent of the test. The exhaustion cannot be attributed to work-hardening during relaxation either, since stress-relaxation tests do not induce significant changes in the sample dimensions;<sup>17,20</sup> in the present situation the plastic strain during relaxation did not exceed 0.0015.

### 3. THE METHOD

#### 3.1. Overall Description

The basic experiment is the determination of sequential relaxation curves from the same reference stress,  $\sigma_R$ . After a fixed relaxation time,  $\tau_i$ , or upon reaching some pre-established relaxed stress level,

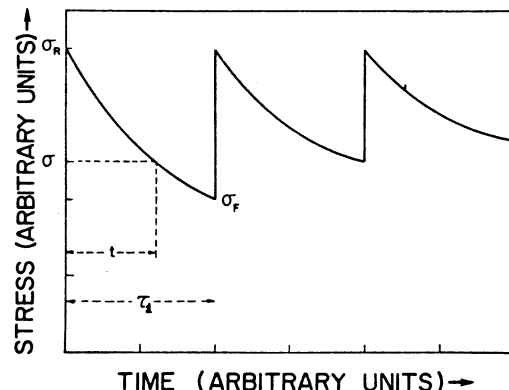


Fig. 6—Schematic stress vs time plot of sequential relaxations showing "exhaustion". Parameters defined:  $\sigma_R$ —reference stress;  $\sigma_F$ —final stress;  $t$ —time,  $\tau_1, \tau_2, \dots, \tau_i$ —times corresponding to full cycles.

the material is reloaded up to  $\sigma_R$  and the procedure is repeated. A possible outcome of such an experiment is schematically displayed in Fig. 6. The relaxation curves were drawn to make exhaustion obvious: notice that the stress relaxed per cycle decreases from cycle to cycle. The following quantities are relevant for the proposed method of analysis: the reference stress,  $\sigma_R$ , the relaxed stress in each cycle,  $\sigma_F$ , the rate of stress decay,  $\dot{\sigma}$ , and the elapsed time after  $i$  full cycles are completed,  $\tau_i$ .

The detection of substructure evolution and, in particular, the time dependence of  $\rho_m$  relatively to its initial value,  $\rho_m(0)$ , may be accomplished by comparing the relaxation rates at the reference stress level in the different cycles. In fact, Orowan's equation<sup>21</sup> states that:

$$\epsilon = \psi b \rho_m(t) \bar{l} \quad [2]$$

where  $\epsilon$  is the strain,  $\psi$  a geometric factor,  $b$  the magnitude of the Burgers vector of the dislocations,  $\rho_m(t)$  the mobile dislocation density, and  $\bar{l}$  the average distance traveled by each dislocation. The time derivative will yield:

$$\dot{\epsilon}(t) = \psi b \rho_m(t) \bar{s} + \psi b \bar{l} \dot{\rho}_m(t) \quad [3]$$

where  $\bar{s}$  is the average velocity. So, the instantaneous strain rate is composed of a term due to the motion of the dislocations and of a second term due to the variation in the mobile dislocation density. It is reasonable to assume that during stress relaxation the first term dominates the second, and one has:

$$\dot{\epsilon}(t) = \psi b \rho_m(t) \bar{s}. \quad [4]$$

Recalling that, at a given temperature and for a given deformation mechanism, the dislocation velocity can be assumed to depend only upon the effective stress,  $\sigma_{eff}$ , and that  $\dot{\sigma}$  is proportional to  $\dot{\epsilon}$  during relaxation,<sup>13</sup> it follows that:

$$\frac{\rho_m(\tau_i)}{\rho_m(0)} = \frac{\dot{\sigma}_R(\tau_i)}{\dot{\sigma}_R(0)} \quad [5]$$

where  $\rho_m(\tau_i)$  is the density of mobile dislocations at time  $\tau_i$  (after  $i$  cycles are completed) and  $\rho_m(0)$  is that value at the onset of relaxation.  $\dot{\sigma}_R(\tau_i)$  and  $\dot{\sigma}_R(0)$  are the corresponding relaxation rates at the same reference stress level,  $\sigma_R$ .

The principal assumptions behind Eq. [5] are those inherent to Orowan's equation and that the kinetics of flow at the reference stress remains the same during the experiment. The internal stress is also taken as a constant. Of course the same hypotheses are attached to the usual methods of analysis of stress-relaxation data.

### 3.2. Determination of the Time Dependence of the Mobile Dislocation Density

The material, Armco magnetic ingot iron (composition given in Section 2) was subjected to annealing at 973 K for 30 min in a salt bath. Flat tensile specimens were machined with a cross section of 18.2 mm<sup>2</sup> and gage length 38 mm, previous to heat treatment. These specimens were then stored at ambient temperature for one week and then loaded at a nominal strain rate of  $6 \times 10^{-6}$  s<sup>-1</sup> in an Instron universal testing machine (using hand tightened wedge-action grips) up to a stress level of 228.6 MN/m<sup>2</sup> and allowed to relax during 600 s. Nine relaxation cycles were performed from that same initial stress. Reloading was accomplished by displacing the cross-head of the machine at the same rate as the initial load was applied. The relevant data were read from the machine chart and processed in a computer to yield the stress and the rate of relaxation throughout the cycles. The characteristics of the machine were assessed by testing a null gage-length specimen. It was observed that the machine relaxation became immediately exhausted (on sequential relaxation), observation which is in agreement with the results of Guin and Pratt.<sup>13</sup> Since correction for machine relaxation is complex and can lead to questionable results, it was decided to exclude from this analysis the data from the first relaxation cycle, for the machine contribution would be exhausted thereafter. This procedure is not considered to hamper the validity of this work since its main purpose was to detect changes in substructure rather than measuring its magnitude.

The plot in Fig. 7 shows the fraction of the initial stress,  $\sigma_R$ , relaxed per cycle of equal duration. It is obvious therefrom that "exhaustion" took place. How-

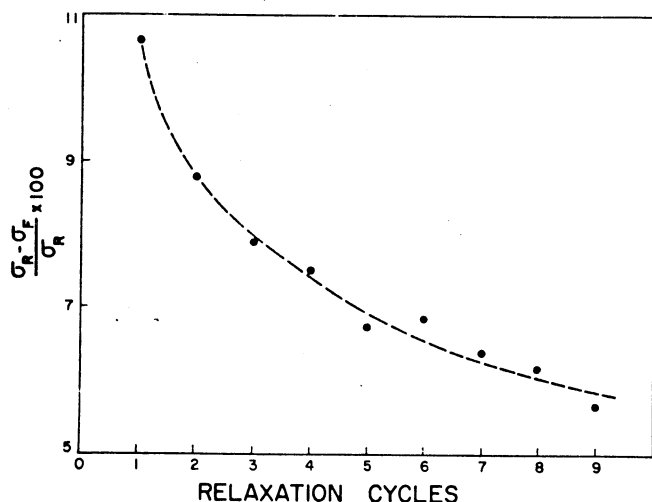


Fig. 7—Percentual relaxation as a function of the number of relaxation cycles for Armco magnetic ingot iron. Data obtained from screw-driven Instron.

ever, it was less rapid than that observed for the same material in Fig. 3. This is thought to be due to the differences in heat treatment times (16 h for Fig. 3 and 30 min for Fig. 7) and/or storing times prior to testing (30 min *vs* seven days). The exhaustion may be caused by either a decrease in  $\rho_m$  or an increase in the internal stress,  $\sigma_i$ , throughout the test. The latter may be discarded because major changes in substructure configuration are not expected to take place. All possible substructural changes—dislocation annihilation, dislocation rearrangement, Snoek atmosphere formation, precipitation at dislocation—would tend to decrease the long-range stresses and, consequently, the internal stress. Because of the very small plastic deformation involved in stress relaxation it is extremely unlikely that dislocation multiplication and long-range dislocation motion—possible contributors to an increase in the internal stress  $\sigma_i$ , are taking place.

The data in Fig. 8 were obtained by applying Eq. [5] to the experimental data. The plot clearly indicates that the density of mobile dislocations would pronouncedly decrease during relaxation. It is noteworthy that after 10 min  $\rho_m$  decreased about 50 pct and after 1 h, 87 pct. These figures would be higher if the first relaxation cycle were considered.

### 3.3. Determination of the Activation Volume

However, in order that the data of Fig. 8 obtained by applying Eq. [5] may be considered truly representative of the time dependence of  $\rho_m$ , it must be confirmed that the same deformation mechanism operates at the onset of each relaxation cycle. Unfortunately this could not be done directly. The validity of the hypothesis of constant deformation mechanism at  $\sigma_R$  was checked by determining the activation volume at the onset of each relaxation cycle.

The activation volume is defined for a constant substructure and assuming first-order kinetics, as (Eq. [8] of Ref. 25 and Eq. [2.4.11] of Ref. 26):

$$v^* = kT \left( \frac{\partial \ln \dot{\gamma}}{\partial \tau} \right)_{T, \text{subst}} \quad [6]$$

$\dot{\gamma}$  is the shear strain rate; it is proportional to  $\dot{\epsilon}$ . For stress relaxation, recalling that  $\dot{\sigma}$  and  $\dot{\epsilon}$  are proportional, and that  $\tau$  (shear stress) can be approximated

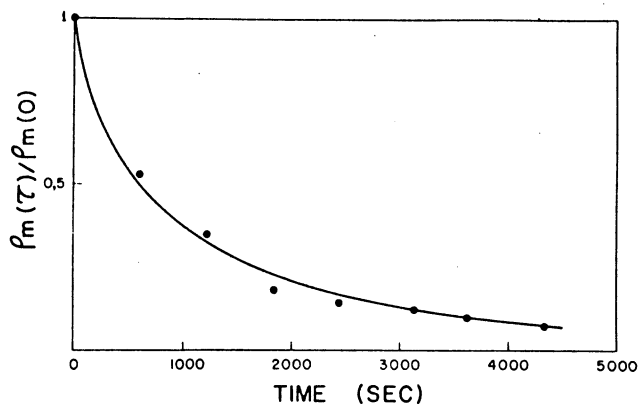


Fig. 8—Time dependence of mobile dislocation density for Armco magnetic ingot iron. Obtained from application of Eq. [5] to Fig. 7.

as  $\sigma/2$ , one has:

$$v^* = 2 kT \left( \frac{\partial \ln \dot{\sigma}}{\partial \sigma} \right)_{T, \text{subst}} \quad [7]$$

Under conditions of variable mobile dislocation density, Eq. [7] has to be adjusted since  $v^*$  expresses the behavior of the individual dislocations. The activation volume is generated by the motion of the individual dislocations and should not be affected by a change in their density, assuming that the velocity of the dislocations is a function only of the applied stress and that the barriers will not be affected by changes in the mobile dislocation density. On the other hand, the plastic strain rate during relaxation,  $\dot{\gamma}$ , is proportional to the mobile dislocation density. Accordingly, Eq. [7] has to be modified if it is applied to situations where the mobile dislocation density is time dependent. This can be done by using Eq. [4], in which the strain rate is related to the average dislocation velocity:

$$\dot{\gamma}(t) = A_1 \dot{\epsilon}(t) = A_1 \psi b \rho_m(t) \bar{s} = A_2 \rho_m(t) \bar{s} \quad [8]$$

$A_1$  and  $A_2$  are constants. When  $\rho_m(t)$  is constant:

$$\dot{\gamma}(t) = A_2 \rho_m(o) \bar{s} \quad [9]$$

When  $\rho_m(t)$  is a function of time, Eq. [9] has to be adjusted so that the term  $A_2 \rho_m(o) \bar{s}$ , which describes the motion of the individual dislocations (through the average velocity  $\bar{s}$ ) remains unchanged. One way of doing this is by multiplying Eq. [8] by  $\rho_m(o)/\rho_m(t)$ :

$$\dot{\gamma}(t) \cdot \frac{\rho_m(o)}{\rho_m(t)} = A_2 \rho_m(o) \bar{s} \quad [10]$$

The right sides of Eqs. [9] and [10] are the same, and  $\dot{\gamma}(t) \rho_m(o)/\rho_m(t)$  can be substituted for  $\dot{\gamma}(t)$  in Eq. [6]:

$$v^* = kT \left[ \frac{\partial \ln \left( \frac{\dot{\gamma}(t)}{\rho_m(t)} \cdot \rho_m(o) \right)}{\partial \tau} \right]_T \quad [11]$$

So,

$$v^* = 2 kT \left[ \frac{\partial \ln \dot{\sigma}(t) - \partial \ln \frac{\rho_m(t)}{\rho_m(o)}}{\partial \sigma} \right]_T \quad [12]$$

In the calculations conducted to determine  $v^*$ , the following parameter was introduced:

$$\phi(t) = \frac{\dot{\sigma}(t)}{\rho_m(t)} \text{ and } \frac{\phi(t)}{\phi(o)} = \frac{\frac{\dot{\sigma}(t)}{\rho_m(t)}}{\frac{\dot{\sigma}(o)}{\rho_m(o)}} = \frac{\dot{\sigma}(t)}{\rho_m(t)} \cdot \frac{\rho_m(o)}{\dot{\sigma}(o)} \quad [13]$$

In terms of  $\phi(t)$ ,  $v^*$  can be expressed as:

$$v^* = 2 kT \left[ \frac{\partial \ln \frac{\phi(t)}{\phi(o)} + \partial \ln \dot{\sigma}(o)}{\partial \sigma} \right]_T \quad [14]$$

Figure 9 shows a plot of  $\ln \phi(t)/\phi(o)$  vs  $\sigma$  for the first relaxation cycle used in the analysis.  $\rho_m(t)/\rho_m(o)$  ratios were obtained from Fig. 8 and  $\dot{\sigma}(t)/\dot{\sigma}(o)$  from the stress-relaxation curve. The initial stress rate for this cycle was  $\dot{\sigma}(o) = -0.0854 \text{ MN/m}^2 \cdot \text{s}$ . The

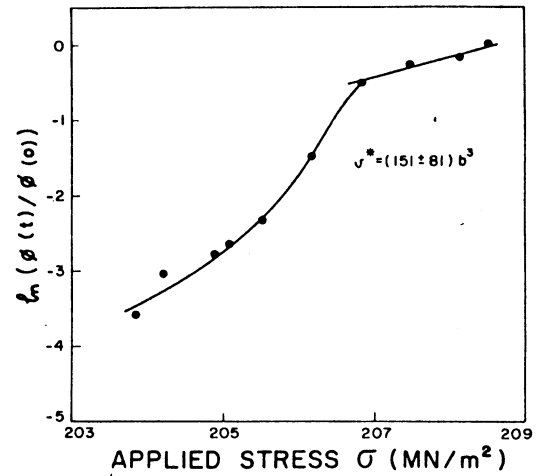


Fig. 9— $\ln [\phi(t)/\phi(o)]$  vs applied stress for the second relaxation cycle in Armco magnetic ingot iron. The slope of the linear portion (at the higher stresses) provides the activation volume for the initial stage of stress relaxation.

corresponding activation volume for the first portion of relaxation (straight line in top right-hand corner of Fig. 9) could therefore be estimated. It was found, with 95 pct confidence, to be  $(151 \pm 83)b^3$ . For iron,  $b$  was taken as  $0.248 \text{ nm}$ .<sup>27</sup> The same type of analysis was repeated for the fourth, sixth and eighth cycles. The values of  $v^*$  obtained were  $(88 \pm 35)b^3$ ,  $(57 \pm 31)b^3$ ,  $(121 \pm 35)b^3$  respectively. The high percentage error in  $v^*$ , probably due to the error in the numerical programming of the data to obtain  $-\dot{\sigma}$ , does not allow the identification of a trend of variation among these figures. That is, if  $v^*$  changes during the test, the detection of this is beyond the precision of our method of data reduction. So, the same deformation mechanism was considered to be operating at the beginning of all relaxation cycles and the time dependence of mobile dislocation density calculated in Section 3.2 and portrayed in Fig. 8 should be valid.

It follows from this analysis that the plot of Fig. 7 may be taken as an indication that the usual assumption, constant  $\rho_m$ , is not adequate and will lead to meaningless conclusions about the behavior of the material. However, the tendency of the plot of Fig. 7 to level off with increasing time suggests that thereafter the usual analysis could be applied with less imprecision. However, data acquisition would become critical.

The observation of a decrease in  $\rho_m$  during stress relaxation of this iron at room temperature can almost be labeled "to be expected". This is so because the interstitial content in it (0.05 at. pct) is enough to effectively interfere with the mobile dislocations due to ordering.<sup>23</sup> This phenomenon, also known as "Snoek effect" amounts to a friction stress additive to other fields opposing the dislocation motion.<sup>21</sup> Thus, these defects are slowed down both by virtue of a decreasing applied stress and by interaction with the stress fields created by the ordered interstitials. Both processes should favor the subsequent locking of the dislocations by interstitial pinning.<sup>24</sup> The occurrence of interstitial ordering at lower stresses is consistent with the abrupt decrease in  $\ln \phi(t)/\phi(o)$  and hence in  $\phi(t)$  at an intermediate stress. The relatively small activation volume characteristic of the short-range

barrier at the onset of relaxation is consistent with overcoming Peierls stress—the most likely rate controlling mechanism of flow in bcc iron at higher stresses.<sup>25</sup> The decrease in  $\ln \phi(t)/\phi(o)$  with decreasing stress indicates that  $v^*$  should increase which should be expected in the case of overcoming Snoek atmospheres to become the critical step to flow. The observation of increasing  $v^*$  with decreasing  $\sigma$  is also consistent with Conrad's results<sup>25</sup> who suggested that Snoek-type ordering could be responsible for that. No attempt was made to determine  $v^*$  for this second mechanism, for it would be a function of the interstitial content in solution which in the present case is assumed to decrease as the dislocations are pinned.

It is important to add that the assumption of invariant dislocation-barrier interactions is implicit in the foregoing analysis.

### 3.4. Comparison of Results with Dislocation Pinning Hypothesis

Again, it is emphasized that the alloy studied in Section 3, Armco magnetic ingot iron, is not ideally suited for this type of experiment. The presence of both carbon and nitrogen as interstitials, in addition to the seven or more different elements in substitutional solid solution might lead to confusing results. Indeed it has been shown by Leslie and coworkers<sup>28-30</sup> that substitutional atoms cause strain aging in iron. Additionally, the possibility of interstitial-substitutional interactions cannot be fully discarded. Accordingly, a rigorous analysis of the phenomena responsible for "exhaustion" would require the preparation of special "academic" alloys. However, this was thought to be beyond the scope of this paper, whose objective is to present a possible correction method and illustrate it by applying it to a real situation.

In order to test the hypothesis that the density of mobile dislocations would be reduced by locking by interstitials a simple model was developed (see Appendix). It follows therefrom that to a first approximation (or reasonably short times) the ratio  $\rho_m(\tau_i)/\rho_m(o)$  should depend upon  $\tau_i$  as:

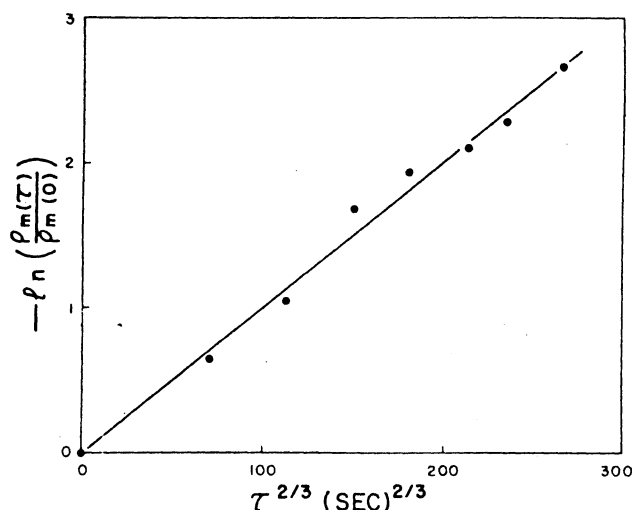


Fig. 10—Comparison of the time dependence of mobile dislocation density on sequential relaxations with predictions from the proposed pinning mechanism.

$$\ln \frac{\rho_m(\tau_i)}{\rho_m(o)} = -\lambda \tau_i^{2/3} \quad [15]$$

where  $\lambda$  is an appropriate constant. The values of  $\rho_m(\tau_i)/\rho_m(o)$  obtained by using Eq. [5] are plotted in Fig. 10, after Eq. [15]. The agreement between the data and the model can be said to be extremely good and supports the initial contention.

An attempt was made to calculate  $\lambda$  (given in Eq. [A.6], Appendix) and to compare it with the value shown in Fig. 10 ( $\lambda = 10^{-2} \text{ s}^{-2/3}$ ). There are uncertainties in Eq. [A.6]:  $N_o$ ,  $\alpha$ ,  $\xi$ ,  $B$ . Values from Bergström and Roberts<sup>33</sup> were used for  $\alpha$  ( $= 1.2$ ),  $\xi$  ( $= 5 \times 10^7 \text{ cm}^{-1}$ ),  $B$  ( $= 1.15 \times 10^{-20} \text{ dyne} \cdot \text{cm}^2$ ),  $D$  ( $= 8.45 \times 10^{-17} \text{ cm}^2 \text{ s}^{-1}$ ). Bergström and Roberts believe that the principal pinning atom is nitrogen, because of its larger solubility in iron. So:

$$\lambda \approx 10^{-16} N_o. \quad [16]$$

Replacing  $\lambda$  by its experimentally observed value ( $10^{-2}$ ) into Eq. [16], one obtains:

$$N_o \approx 10^{14}. \quad [17]$$

This corresponds to an atomic fraction of approximately  $10^{-9}$ , orders of magnitude below the carbon plus nitrogen atomic fraction (approximately  $5 \times 10^{-4}$ ).

Truly it is important to notice that the association of the decrease in  $\rho_m$  to interstitial pinning does not necessarily imply that the thermal component of the flow stress, for this iron, is determined by interstitial dragging. However, if information about the kinetics of flow were to be obtained from the relaxation curves the aging effect should be taken into account for the relaxation process is obviously controlled by at least two parallel reactions.

## 4. CONCLUSIONS

1) Two simple tests were proposed to verify whether the mechanical response of the substructure remains constant during relaxation. These tests consist of a) subjecting the sample to repeated relaxation cycles from a same reference stress and b) observing whether a yield point forms on reloading after the last relaxation cycle.

2) These tests were applied to four different metal systems at ambient temperature. It was found that, for 99.999 pct copper the mobile dislocation density remains constant. On the other hand, there is both exhaustion of relaxation (on repeated cycling) and yield-point formation for 6061-T6 aluminum, Armco magnetic ingot iron, and an Fe-31 pct Ni-0.1 pct C alloy. The latter effects are indicative of a decrease in mobile dislocation during relaxation.

3) A method for the obtention of the time dependence of mobile dislocation density,  $\rho_m$ , was presented on the assumption that a decrease in  $\rho_m$  is responsible for the "exhaustion" of relaxation on repeated cycling. The time dependence of mobile dislocations, as a fraction of their initial value, was obtained for Armco magnetic ingot iron.

4) The exhaustion of relaxation in Armco magnetic ingot iron was correlated with pinning of dislocations by interstitial atoms. This was done by adapting Cottrell-Bilby-Harper's equation for pinning of dislocations by interstitials to the conditions imposed by

stress-relaxation testing (constant total dislocation density). The decrease in mobile dislocation density throughout the several cycles was found to be adequately explained by assuming classical interstitial pinning.

## APPENDIX

The development of Eq. [15] in the text was based upon the following assumptions:

i) The total dislocation density in the material,  $\rho_o$ , remains constant during relaxation, which is reasonable, since the extent of the concurrent plastic deformation is minimum.

ii) Dislocation remobilization does not occur, which is also reasonable, since during the test the applied stress is always equal or less than the initially applied stress. Annihilation is also ignored.

iii) The Cottrell-Bilby-Harper model<sup>31,32</sup> describes adequately the aging process.

If interstitials are needed to immobilize a dislocation and admitting a uniform distribution of both the dislocations and the interstitials, the rate of dislocation immobilization will be:

$$\frac{d\rho_i}{dt} = \frac{\rho_m}{\xi\rho_o} \frac{dN}{dt} \quad [A.1]$$

where  $N$  is the number of interstitials per unit volume of solution and  $t$  stands for time;  $\xi$ , the number of interstitial atoms per unit length required to completely lock a dislocation, is equal to  $z/d$ , where  $d$  is the distance between atom planes along the dislocation line and  $z$  is the number of interstitials per atom plane required to completely lock the dislocation;  $\rho_i$  and  $\rho_m$  are the densities of immobile and mobile dislocations, respectively. It is implicit in Eq. [A.1] that the interstitials will diffuse with equal probability to all dislocations in the material. The possibility of local saturation was not taken into account.

Since  $\rho_i$  and  $\rho_m$  are related through  $\rho_o = \rho_i + \rho_m = \text{constant}$ ,

$$\frac{d\rho_i}{dt} = -\frac{d\rho_m}{dt} \quad [A.2]$$

From the Cottrell-Bilby-Harper<sup>31,32</sup> model, it is possible to write:

$$\frac{dN}{dt} = (N_o - N) \alpha \left(\frac{BD}{kT}\right) \rho_o t^{-1/3} \quad [A.3]$$

where  $N_o$  is the total amount of interstitials initially available,  $D$  is the diffusion coefficient of the interstitial, and  $\alpha$  and  $B$  are constants related to the types of dislocations and solute atom;  $k$  and  $T$  have the usual meanings.

Substituting Eqs. [A.2] and [A.3] in Eq. [A.1] and performing the integration from  $t = 0$  to  $\tau$  yields

$$\ln \frac{\rho_m(\tau_i)}{\rho_m(0)} = -\left(\frac{N_o}{\xi\rho_o}\right) \left(\frac{3}{2}\right) \left[1 - \exp - \alpha \left(\frac{BD}{kT}\right)^{2/3} \rho_o \tau_i^{2/3}\right] \quad [A.4]$$

This equation, for small values of the exponential argument can be written simply as:

$$\ln \frac{\rho_m(\tau_i)}{\rho_m(0)} = -\lambda \tau_i^{2/3} \quad [A.5]$$

where,

$$\lambda = \frac{3}{2} \cdot \frac{N_o}{\xi} \cdot \alpha \left(\frac{BD}{kT}\right)^{2/3} \quad [A.6]$$

## ACKNOWLEDGMENTS

This work was partly supported by the Brazilian Army through IME Materials Research Center. One of us (M.A.M.) would like to thank the South Dakota School of Mines and Technology and University of Denver for the provision of facilities. Thanks are also due to Mr. A. R. Pelton for experimental help, to Dr. Bruce R. Palmer for helpful discussions, and to Professor J. D. Embury for helpful discussions during the revision of this manuscript. The copper specimens were kindly provided by Dr. T. R. Homa, I.B.M.-Endicott.

## REFERENCES

1. J. C. M. Li: *Can. J. Phys.*, 1967, vol. 45, p. 493.
2. I. Gupta and J. C. M. Li: *Met. Trans.*, 1970, vol. 1, p. 2323.
3. H. Conrad: *Mater. Sci. Eng.*, 1970, vol. 2, p. 265.
4. A. S. Krausz and H. Eyring: *Deformation Kinetics*, p. 226, Wiley Interscience, NY, 1975.
5. W. G. Johnston and J. J. Gilman: *J. Appl. Phys.*, 1959, vol. 30, p. 129.
6. A. S. Krausz: *Mater. Sci. Eng.*, 1976, vol. 22, p. 91.
7. R. W. Rohde and T. V. Nordstrom: *Scr. Met.*, 1973, vol. 7, p. 317.
8. K. Okazaki, Y. Aono, and M. Kagawa: *Acta Met.*, 1976, vol. 24, p. 1121.
9. B. J. Shaw and G. A. Sargent: *Acta Met.*, 1964, vol. 12, p. 1225.
10. K. Tangri and D. J. Lloyd: *J. Appl. Phys.*, 1974, vol. 45, p. 4268.
11. D. J. Lloyd and J. D. Embury: *Phys. Status Solidi (b)*, 1971, vol. 43, p. 393.
12. J. R. C. Guimarães and M. A. Meyers: *Scr. Met.*, 1977, vol. 11, p. 193.
13. F. Guin and P. L. Pratt: *Phys. Status Solidi*, 1964, vol. 6, p. 111.
14. G. B. Gibbs: *Phil. Mag.*, 1966, vol. 13, p. 317.
15. P. P. Gillis and R. E. Medrano: *J. Mater.*, 1971, vol. 6, p. 514.
16. M. A. Meyers and J. R. C. Guimarães: *32nd Annual Meeting of the Brazilian Society for Metals*, São Paulo, Brasil, July 1977.
17. G. F. Bolling: *Phil. Mag.*, 1969, vol. 19, p. 537.
18. J. M. Roberts and W. S. Owen: *Dislocation Dynamics*, A. R. Rosenfield, G. T. Hahn, A. L. Bement, Jr., and R. I. Jaffee, eds., pp. 357-79, McGraw-Hill, NY, 1968.
19. C. L. Magee and H. W. Paxton: *Trans. TMS-AIME*, 1968, vol. 242, p. 1741.
20. A. R. C. Westwood and T. Broom: *Acta Met.*, 1957, vol. 5, p. 77.
21. E. Orowan: *Proc. Phys. Soc.*, 1940, vol. 52, p. 8.
22. A. W. Cocharde, G. Schoeck, and H. Wiedersich: *Acta Met.*, 1955, vol. 3, p. 533.
23. G. Schoeck and A. Seeger: *Acta Met.*, 1959, vol. 7, p. 469.
24. H. Conrad: *JISI*, 1961, vol. 194, p. 364.
25. H. Conrad: *J. Metals*, 1964, vol. 16, p. 582.
26. Source cited in Ref. 4, p. 120.
27. H. Conrad and W. Hayes: *Trans. ASM*, 1963, vol. 56, p. 249.
28. W. B. Morrison and W. C. Leslie: *JISI*, 1973, vol. 211, p. 129.
29. C. C. Li and W. C. Leslie: *Met. Trans. A*, 1975, vol. 6A, p. 1987.
30. C. C. Li, J. Dziura, and W. C. Leslie: *Met. Trans. A*, 1977, vol. 8A, p. 705.
31. A. H. Cottrell and B. A. Bilby: *Proc. Phys. Soc.*, 1949, vol. A62, p. 49.
32. S. Harper: *Phys. Rev.*, 1951, vol. 83, p. 709.
33. Y. Bergström and W. Roberts: *Acta Met.*, 1971, vol. 19, p. 1243.
34. K. Okazaki, Y. Aono, T. Kanciyuki, and H. Conrad: *Mater. Sci. Eng.*, 1978, vol. 33, p. 253.